

Transverse Momentum Distribution in $\Psi(1S, 2S)$ Photoproduction in PP and AA Collisions at the LHC

Sony Martins and Maria Beatriz de Leone Gay Ducati

Instituto de Física

Universidade Federal do Rio Grande do Sul (UFRGS)

Av. Bento Gonçalves, 9500 - Agronomia, Porto Alegre - RS, 91501-970, Brazil

sony.martins@ufrgs.br, beatriz.gay@ufrgs.br

Published 15 August 2017

The exclusive photoproduction of the heavy vector mesons $\Psi(1S, 2S)$ is investigated in the context of ultra-peripheral collisions proton-proton and nucleus-nucleus for the energies available at the LHC run 2. Using the light-cone color dipole formalism, it was calculated the transverse momentum distribution in the central rapidity region, in which it is expected major contribution for the process.

Keywords: Ultra-Peripheral, Photoproduction, Heavy Vector Mesons.

PACS numbers: 12.39.St, 13.85

1. Introduction

In the ultra-peripheral collisions regime ¹ (impact parameter $b > 2R_A$), the exclusive photoproduction dominates the process through the emission of virtual photons that interact with the target. The photoproduction provides ways to investigate the transition between the linear and the non-linear dynamics, characterized by the limitation on the maximum phase-space parton density that can be reached in the hadron wave-function (saturation phenomenon ^{2,3}). The theoretical framework considered in the analysis is the light-cone color dipole formalism ⁴, which includes consistently both the parton saturation effects in photon-proton interaction as nuclear shadowing effects in photon-nucleus process.

In this work, it was investigated the transverse momentum distribution ⁵ for the exclusive photoproduction of mesons $\Psi(1S, 2S)$ in proton-proton ($\sqrt{s} = 13$ TeV) and nucleus-nucleus ($\sqrt{s} = 5.5$ TeV) collisions in the LHC energy interval (Run 2).

This is an Open Access article published by World Scientific Publishing Company. It is distributed under the terms of the Creative Commons Attribution 4.0 (CC-BY) License. Further distribution of this work is permitted, provided the original work is properly cited.

2. Theoretical Framework

In the ultra-peripheral regime, the rapidity distribution of the vector meson in pp collisions is given by ^{6,7}

$$\frac{d\sigma}{dy} (p + p \rightarrow p + p + V) = S_{gap}^2 \left[\omega \frac{dN_\gamma^p(\omega)}{d\omega} \sigma(\gamma p \rightarrow V + p) + (y \rightarrow -y) \right], \quad (1)$$

where the first term, $dN(\omega)/d\omega$, represents the virtual photons flux, calculated from the Weizsäcker Williams method ⁸ and the second term, $\sigma_\gamma^p(\omega)$, it is the photoproduction cross section that quantifies the cross section for the $\gamma + p \rightarrow p + \Psi_{(1S,2S)}$ process. The parameter S_{gap}^2 estimates the absorptive corrections and, here, it is taken the average value $S_{gap}^2 = 0.8$ (see Ref. ²⁰). In the present work, we considered the color dipole approach for modeling the photoproduction cross section,

$$\sigma(\gamma p \rightarrow V p) (s, Q^2) = \frac{1}{16\pi B_V} \left| \int d^2 \mathbf{r} \int_0^1 \frac{dz}{4\pi} \rho_V(z, r) A_{q\bar{q}}(x, r, \Delta = 0) \right|^2 (1 + \beta^2) R_g(\lambda_{eff}). \quad (2)$$

The parameter B_V (slope parameter) was calculated from the Regge phenomenology ¹⁰ with the energy dependence. The parameters $\beta = \text{Re}A/\text{Im}A$ and R_g corresponds, respectively, the real contribution of the frontal amplitude and off-diagonal momenta of exchanged gluons (skewedness effect). The function $\rho_V = (\Psi_V^* \Psi)_T$ corresponds to overlap of the photon-meson wave functions ¹¹, while the amplitude $A_{q\bar{q}}$ represents the dipole-target scattering amplitude (assumed to be imaginary). Finally, the variables z and r are the longitudinal momentum fraction carried by the quark and the transverse color dipole size, respectively.

To model the meson wave-function, it was used the Boosted-Gaussian model ¹¹ since it can be applied in a systematic way for excited states. The parameters \mathcal{R}_{nS}^2 and \mathcal{N}_{nS} presented in the model were calculated in ^{12,13}. Other important component in Eq. (2) is the dipole scattering amplitude, which is related to the color dipole cross section in the form

$$\sigma_{q\bar{q}}(x, r) = 2 \int d^2 b A_{q\bar{q}}(x, r, b),$$

bearing in mind that b and Δ are Fourier conjugates variables. We considered the models GBW ¹⁴ and GBW-KSX (see Ref. ¹⁵), which the last takes into account the effect of the gluon number fluctuations. It was also considered the CGC model ¹⁶, labeled for CGC-old parameterization ¹⁷ which considers the previous DESY-HERA data and CGC-new ¹⁸ which considers more recent data from ZEUS and H1 combined results for inclusive DIS. Finally, it was included the b-CGC model ¹⁹, with impact parameter dependence in the dipole-proton scattering amplitude.

In the case of nuclear targets, the coherent photonuclear cross section was calculated using the expression ²¹,

$$\sigma(\gamma A \rightarrow V A)(\omega) = R_g^2 \frac{|A_{nuc}(x, \Delta = 0)|^2}{16\pi} (1 + \beta^2) \int_{t_{min}}^{\infty} |F(t)|^2 dt,$$

where

$$t_{min} = (m_V^2 / 2\omega)^2$$

and the nuclear form factor is given by

$$F(q) = \frac{4\pi\rho_0}{Aq^3} [\sin(qR_A) - qR_A \cos(qR_A)] \left[\frac{1}{1 + a^2q^2} \right],$$

with $q = \sqrt{|t|}$, $\rho_0 = 0.1385 \text{ fm}^{-3}$ and $a = 0.7 \text{ fm}$.

3. Results and Discussions

To test the precision of the models, it was calculated the rapidity distribution in order to compare with the available data of LHC for the J/ψ and $\Psi(2S)$ production in $\sqrt{s} = 7 \text{ TeV}$, Figures 1 and 2.

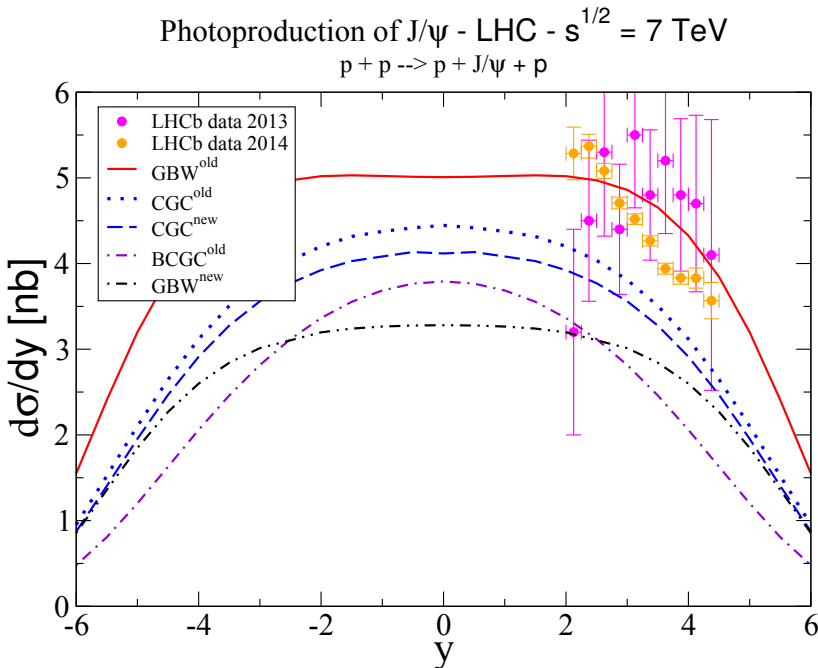


Fig. 1. Rapidity distribution for the vector meson states $\Psi(1S)$ in pp collisions in the LHC Run I at $\sqrt{s} = 7 \text{ TeV}$.

The relative normalization and the overall behavior on rapidity are well reproduced by all the models in the forward region in comparison to the experimental results from LHCb Collaboration. However, due to the limited experimental data, we can not discard the dipole models for the exclusive photoproduction of the J/ψ and $\psi(2S)$.

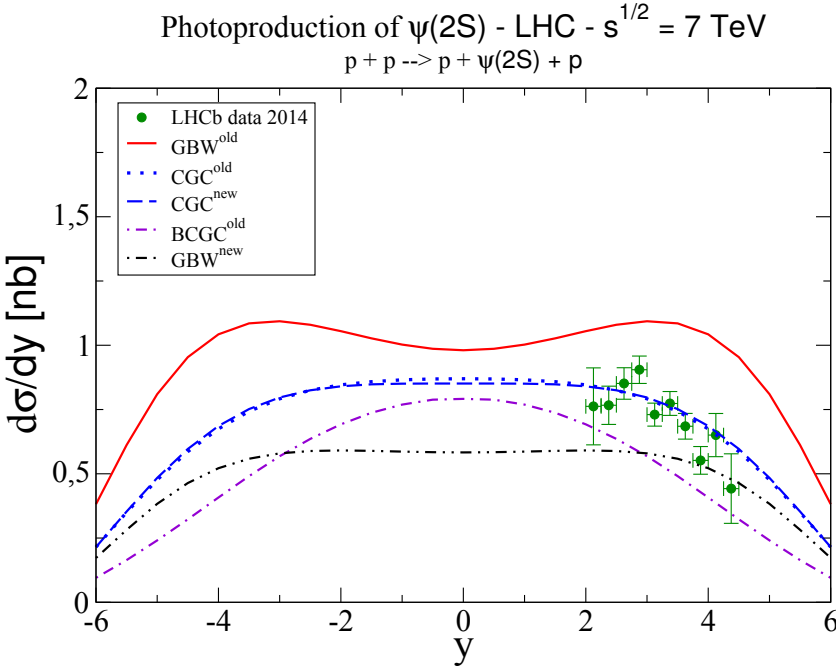


Fig. 2. Rapidity distribution for the vector meson states $\Psi(2s)$ in pp collisions in the LHC Run I at $\sqrt{s} = 7$ TeV.

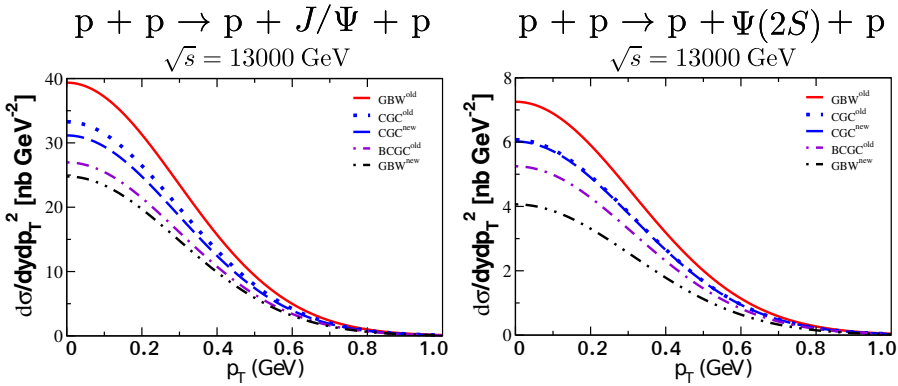


Fig. 3. Results for the p_T distribution of the $\Psi(1S, 2S)$ states in pp collision at $\sqrt{s} = 13$ TeV.

Using the central results ($y = 0$) of the rapidity distribution at $\sqrt{s} = 13$ TeV, it was calculated the p_T -distribution for the vector mesons $\Psi(1S, 2S)$ in pp and AA collisions. First, in pp collision case, the p_T -distribution is given, approximately, by

$$\frac{d^2\sigma}{dy dp_T^2} \Big|_{y=0} \approx \frac{d\sigma}{dy} \Big|_{y=0} B_V(y=0) e^{-B_V p_T^2},$$

from which estimates for pp collision corresponding the production of the $\Psi(1S, 2S)$ at $\sqrt{s} = 13$ TeV, Fig. 3. It was obtained the Gaussian behavior consistent with the exponential ansatz, $A_{qq} \propto e^{-B_V \Delta^2/2}$, applied in the DESY-HERA experimental data on vector meson photoproduction. On the other hand, for the PbPb collision, the momentum transverse distribution in the central region ($y = 0$) is given by

$$\frac{d^2\sigma}{dydp_T^2} \Big|_{y=0} = \frac{\frac{d\sigma}{dy} \Big|_{y=0} \left| F(|t| = p_T^2) \right|^2}{\int_{-\infty}^{t_{min}} \left| F(|t| = p_T^2) \right|^2 dt},$$

with

$$t_{min} = \left(\frac{m_V^2}{4\omega} \right)^2.$$

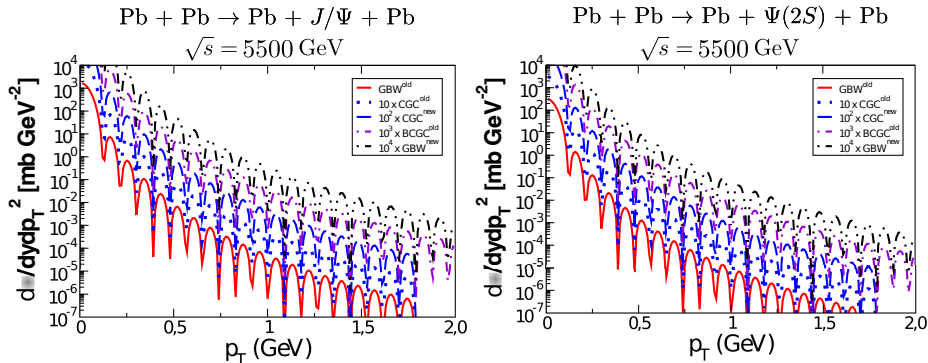


Fig. 4. Results for the p_T distribution of the $\Psi(1S, 2S)$ states in PbPb collision at $\sqrt{s} = 5.5$ TeV.

In this case, it were obtained the results of the Fig. 4, where the form factor used gives rise to oscillatory behavior that is a characteristic of diffractive processes.

References

1. G. Baur, K. Hencken, D. Trautmann, S. Sadovsky, and Y. Kharlov, *Phys. Rep.* **364**, 359 (2002). C. A. Bertulani, S. R. Klein, and J. Nystrand, *Ann. Rev. Nucl. Part. Sci.* **55**, 271 (2005).
2. F. Gelis, E. Iancu, J. Jalilian-Marian, and R. Venugopalan, *Ann. Rev. Nucl. Part. Sci.* **60**, 463 (2010). H. Weigert, *Prog. Part. Nucl. Phys.* **55**, 461 (2005). J. Jalilian-Marian and Y. V. Kovchegov, *Prog. Part. Nucl. Phys.* **56**, 104 (2006).
3. M. B. Gay Ducati, *Braz. J. Phys.*, v. **31**, 115 (2001). A. Ayala, M. B. Gay Ducati, and E. M. Levin, *Eur. Phys. J. C* **8**, 115 (1999). A. Ayala, M. B. Gay Ducati, and E. M. Levin, *Phys. Lett. B* **388**, 188 (1996). A. Ayala, M. B. Gay Ducati, and E. M. Levin, *Nucl. Phys. B* **493**, 305 (1997). A. Ayala, M. B. Gay Ducati, and E. M. Levin, *Nucl. Phys. B* **511**, 355 (1998).
4. N. N. Nikolaev, B. G. Zakharov, *Phys. Lett. B* **332**, 184 (1994). *Z. Phys. C* **64**, 631 (1994).

5. M. B. Gay Ducati, F. Kopp, M. V. T. Machado, and S. Martins, *Phys. Rev. D* **94**, 094023 (2016).
6. M. B. Gay Ducati, M. T. Griep, and M. V. T. Machado, *Phys. Rev. D* **88**, 017504 (2013).
7. M. B. Gay Ducati, M. T. Griep, and M. V. T. Machado, *Phys. Rev. C* **88**, 014910 (2013).
8. G. Baur *et al.*, *Phys. Rep.* **364**, 359 (2002). C. A. Bertulani, S. R. Klein, and J. Nystrand, *Ann. Rev. Nucl. Part. Sci.* **55**, 271 (2005).
9. W. Schäfer and A. Szczurek, *Phys. Rev. D* **76**, 094014 (2007).
10. G. S. Santos and M. V. T. Machado, *J. Phys. G* **42**, 105001 (2015).
11. J. Nemchik, N. N. Nikolaev, E. Predazzi, and B. G. Zakharov, *Z. Phys. C* **75**, 71 (1997).
12. N. Armesto and A. H. Rezaeian, *Phys. Rev. D* **90**, 054003 (2014).
13. B.E. Cox, J. R. Forshaw, and R. Sandapen, *JHEP* **0906**, 034 (2009).
14. K. Golec-Biernat and M. Wüsthoff, *Phys. Rev. D* **59**, 014017 (1998).
15. M. Kozlov, A. Shoshi, and W. Xiang, *JHEP* **0710**, 020 (2007).
16. E. Iancu, K. Itakura, and S. Munier, *Phys. Lett. B* **590**, 199 (2004).
17. G. Soyez, *it Phys. Lett. B* **655**, 32 (2007).
18. A. H. Rezaeain and I. Schmidt, *Phys. Rev. D* **88**, 074016 (2013).
19. H. Kowalski, L. Motyka, and G. Watt, *Phys. Rev. D* **74**, 074016 (2006).
20. W. Schafer and A. Szczurek, *Phys. Rev. D* **76**, 094014 (2007).
21. S. Klein and J. Nystrand, *Phys. Rev. C* **60**, 014903 (1999).